Experimental demonstration of the relative phase operator

Alexei Trifonov†‡, Tedros Tsegaye†, Gunnar Björk†¶, Jonas Söderholm†, Edgard Goobar†, Mete Atatüre§ and Alexander V Sergienko‖

† Department of Electronics, Royal Institute of Technology (KTH), Electrum 229, SE-164 40 Kista, Sweden
‡ Ioffe Physical Technical Institute, 26 Polytekhnicheskaya, 194021 St Petersburg, Russia
§ Quantum Imaging Laboratory, Department of Physics, Boston University, 8 Saint Mary's Street, Boston, MA 02215, USA
‖ Quantum Imaging Laboratory, Department of Electrical and Computer Engineering, Boston University, 8 Saint Mary's Street, Boston, MA 02215, USA

E-mail: `gunnarb@ele.kth.se`

Abstract. We have experimentally demonstrated a realization of the two-mode relative phase operator introduced by Luis and Sánchez-Soto (Luis A and Sánchez-Soto L L 1993 *Phys. Rev.* A **48** 4702). The relative phase distribution function was measured for a weakly excited relative phase eigenstate and weakly excited two-mode coherent states. The experiment is also (using the eigenstates) a demonstration of Heisenberg-limited interferometry.

1. Introduction

An outstanding problem in quantum mechanics is the search for a phase operator [1–7]. A number of theories for such an operator have been proposed, (for three recent reviews see [8–10]) but most of them succumb to one or more of three shortcomings: (1) the operator is non-Hermitian; (2) no scheme for an experimental realization (and hence experimental test of the theory) has been suggested; (3) the operator is operationally defined, leaving the questions open as to what observable the measurement apparatus really represents and to what the conjugate observable is.

Most of the work on finding a proper description of quantum phase has assumed that the quantum phase operator is a single-mode operator. However, such an operator cannot be simultaneously Hermitian and work in an unrestricted Hilbert space [11]. Lately, work on finding the operator corresponding to the relative phase between two harmonic oscillators has been undertaken [7, 12–14]. Recently we suggested an experimental implementation [15] of a generalization of the relative phase operator derived by Luis and Sánchez-Soto [12]. Here we report the first experimental confirmation of a quantum relative phase measurement in the spirit of [12, 15].

Before venturing further, let us comment briefly on the name 'relative phase operator'. The operator we call the

¶ Author to whom correspondence should be addressed.

relative phase operator has previously been called the phase-difference operator by us [15] and by others [4,5,8,9,12,14]. However, phase difference implies the difference between two phases. As can be seen from the entangled form of the operator eigenstates (see (2), below) the operator does not represent the difference between the phase of two individual oscillators. In particular, as pointed out by Yu [14, 16] the phase difference between three oscillators 1, 2 and 3 does not fulfil the relation $\hat{\Phi}_{12} + \hat{\Phi}_{23} + \hat{\Phi}_{31} = 0$. For this reason, and also due to the suggestion of one of the reviewers of this paper, we deviate from the established notation and call the operator by a different, but perhaps more appropriate name, than initially given to it by those who first constructed it mathematically [12]. We hope other authors will follow suit.

The outline of the paper is as follows. In section 2, we give a brief introduction to the generalized two-mode relative phase operator and its eigenstates. We also define the relative phase distribution function. In section 3 we delineate how to implement a relative phase analyser using only linear optical components. In section 4 we discuss how we have experimentally implemented the analyser in terms of a polarization interferometer. In section 5 we discuss the generation of relative phase eigenstates and the subsequent detection of the relative phase distribution function of these eigenstates and weak coherent states. This section contains the main results and here the experimental conditions are also described in some detail. Finally, in section 6, we discuss our

results and their interpretation and point to some possible future directions and applications.

2. The relative phase eigenstates and the relative phase operator

The basis for Luis and Sánchez-Soto's relative phase operator [12] is the normalized two-mode state

$$|\phi_{\mathrm{PB}}^{(N)}\rangle = \frac{1}{(N+1)^{1/2}} \sum_{n=0}^{N} |n, N-n\rangle, \qquad (1)$$

where the abbreviated notation $|m, n\rangle \equiv |m\rangle \otimes |n\rangle$ has been used. The state is the two-mode generalization of the Pegg–Barnett single-mode phase eigenstates. The state (1) is a special case of a two-mode equipartition state which can be written

$$|\phi^{(N)}\rangle = \frac{1}{(N+1)^{1/2}} \sum_{n=0}^{N} \exp(\mathrm{i}\theta_n)|n, N-n\rangle, \qquad (2)$$

where θ_n are arbitrary real numbers. It is to be noted that (2), and hence (1), are eigenstates to the total excitation operator $\hat{n}_1 + \hat{n}_2$, where e.g. $\hat{n}_1$ is the number operator operating on the left state in the two-mode bras and kets.

The relative phase shifting unitary operator in 'symmetric' form can be written

$$\mathrm{e}^{\mathrm{i}\phi(\hat{n}_1 - \hat{n}_2)/2} \equiv \mathrm{e}^{\mathrm{i}\phi\hat{n}_{12}}, \qquad (3)$$

where ϕ is a real number and $\hat{n}_{12} \equiv (\hat{n}_1 - \hat{n}_2)/2$ is the number-difference operator. The operator (3) will increase the relative phase between the two modes. It is trivial to show that if

$$\phi = \phi_r^{(N)} = \theta + \frac{2\pi r}{N+1}, \qquad (4)$$

where θ is an arbitrary real number, and $r = 0, 1, \ldots, N$, the states $\exp(\mathrm{i}\phi_r^{(N)}\hat{n}_{12})|\phi^{(N)}\rangle$ and $\exp(\mathrm{i}\phi_k^{(N)}\hat{n}_{12})|\phi^{(N)}\rangle$ are orthogonal for all integers $0 \leqslant r \neq k \leqslant N$. Therefore, in excitation manifold N, where $N + 1$ orthonormal two-mode states exist, a complete orthonormal basis can be generated from a state of type (2) by simply increasing the differential phase shift between the two modes. We define the relative phase eigenstates as the particular set of equipartition states where

$$|\phi_r^{(N)}\rangle = \mathrm{e}^{\mathrm{i}\phi_r^{(N)}\hat{n}_{12}}|\phi^{(N)}\rangle. \qquad (5)$$

Note that the definition is non-unique. In order for the definition to be meaningful both the state $|\phi^{(N)}\rangle$ and the reference angle θ must first be defined.

Since the states $|\phi_r^{(N)}\rangle$ and $|\phi_{r+1}^{(N)}\rangle$ are orthogonal, a differential phase shift as small as $\phi = 2\pi/(N+1)$ can in principle be detected with certainty. Therefore, the relative phase eigenstates allow interferometry with Heisenberg scaling ($\phi_{\min} \propto 1/N$).

Luis and Sánchez-Soto suggested a relative phase operator defined by

$$\hat{\Phi}_{12} \equiv \sum_{N=0}^{\infty} \sum_{r=0}^{N} \phi_r^{(N)} \mathrm{e}^{\mathrm{i}\phi_r^{(N)}\hat{n}_{12}} |\phi_{\mathrm{PB}}^{(N)}\rangle \langle \phi_{\mathrm{PB}}^{(N)}| \mathrm{e}^{-\mathrm{i}\phi_r^{(N)}\hat{n}_{12}}, \qquad (6)$$

which is a special, but important, form of the more general relative phase operator

$$\hat{\Phi}_{12} \equiv \sum_{N=0}^{\infty} \sum_{r=0}^{N} \phi_r^{(N)} \mathrm{e}^{\mathrm{i}\phi_r^{(N)}\hat{n}_{12}} |\phi^{(N)}\rangle \langle \phi^{(N)}| \mathrm{e}^{-\mathrm{i}\phi_r^{(N)}\hat{n}_{12}}. \qquad (7)$$

We define the relative phase distribution function $P_{|\psi\rangle}^{(N)}(\phi_{12})$, where N denotes the manifold, of the two-mode state $|\psi\rangle$ by

$$P_{|\psi\rangle}^{(N)}(\phi_{12}) = |\langle\psi| \exp(\mathrm{i}\phi_{12}\hat{n}_{12})|\phi^{(N)}\rangle|^2. \qquad (8)$$

(Note that the function is similar to, but has a different normalization from, that defined in [12].) The function is 2π-periodic in ϕ_{12}. We see that it is obtained by imposing a (negative) incremental relative phase ϕ_{12} to the state $|\psi\rangle$ and then projecting it onto the state $|\phi^{(N)}\rangle$. In the following we have abbreviated the notation by suppressing the subscript 12 in ϕ_{12}.

We recently suggested that a way of measuring relative phase was to construct a measurement procedure consisting of an energy-conserving unitary rotation of the state, followed by photo-detection [15]. The proper unitary transformation

$$\hat{U} = \sum_{N=0}^{\infty} \sum_{r=0}^{N} |r, N-r\rangle \langle \phi^{(N)}| \mathrm{e}^{-\mathrm{i}\phi_r^{(N)}\hat{n}_{12}} \qquad (9)$$

will project each relative phase eigenstate onto a two-mode photon number-difference state which can be detected using two single-photon resolution photodetectors. As shown in [15] it will be difficult both to generate the states (2) and to construct the associated unitary operator (9) due to the fact that they are maximally entangled states of a particular form. However, since *any* two-mode equipartition state can be used to generate a complete relative phase basis in a particular manifold it is tempting to try to synthesize such a state using two-mode number states and some simple, experimentally realizable, Hamiltonian. In the following we will show how this can be done in the second manifold, which is the lowest nontrivial excitation manifold. (In the first manifold the relative phase measurement corresponds to the single-photon interference experiment performed by Grangier *et al* [17].)

3. Generation and analysis of relative phase eigenstates

In the second photon number manifold we will define the number-difference states $|0, 2\rangle$, $|1, 1\rangle$ and $|2, 0\rangle$ as our basis states, in the delineated order. The unitary matrix corresponding to a differential phase shift between the modes in the given basis is

$$U_{\mathrm{PS}} = \begin{bmatrix} \exp(-\mathrm{i}\phi) & 0 & 0 \\ 0 & 1 & 0 \\ 0 & 0 & \exp(\mathrm{i}\phi) \end{bmatrix}. \qquad (10)$$

The unitary transformation matrix of a beam splitter in the second manifold and in the chosen basis is

$$U_{\mathrm{BS}} = \begin{bmatrix} \cos^2(\xi) & \frac{-\mathrm{i}\sin(2\xi)}{\sqrt{2}} & -\sin^2(\xi) \\ \frac{-\mathrm{i}\sin(2\xi)}{\sqrt{2}} & \cos(2\xi) & \frac{-\mathrm{i}\sin(2\xi)}{\sqrt{2}} \\ -\sin^2(\xi) & \frac{-\mathrm{i}\sin(2\xi)}{\sqrt{2}} & \cos^2(\xi) \end{bmatrix}, \qquad (11)$$

where $\cos^2(\xi)$ is the transmittivity of the beam splitter. By inspection of (11) we see that it is not possible to construct a relative phase eigenstate by using the input state $|0, 2\rangle$ (nor $|2, 0\rangle$, by symmetry) but that it is possible by using the $|1, 1\rangle$ input state if $\xi = \arccos(\pm 1/\sqrt{3})/2 \approx 27.4°$ and $62.6°$ corresponding to beam splitter transmittivities of 78.9% and 21.1%, respectively.

Choosing $\xi = \arccos(1/\sqrt{3})/2$ will yield the state

$$|\phi^{(2)}\rangle = (-i|0, 2\rangle + |1, 1\rangle - i|2, 0\rangle)/\sqrt{3}. \quad (12)$$

This state has the proper form (2) of a relative phase eigenstate.

We have now shown how to construct a two-mode relative phase eigenstate by letting a $|1, 1\rangle$-state impinge on a suitably chosen beam splitter. Conversely, a beam splitter with $\xi = -\arccos(1/\sqrt{3})/2$ will unitarily transform the state (12) to the state $|1, 1\rangle$ which can be detected by recording photo-detector coincidence counts between the two output modes of this beam splitter. Note that such a beam splitter will transform the two orthogonal two-mode relative phase eigenstates to

$$\exp(\pm i2\pi\hat{n}_{12}/3)|\phi^{(2)}\rangle \rightarrow \frac{\pm(1 - \sqrt{3}) - i(1 + \sqrt{3})}{4}|0, 2\rangle$$

$$+ \frac{\mp(1 + \sqrt{3}) + i(\sqrt{3} - 1)}{4}|2, 0\rangle. \quad (13)$$

Measuring these two states with a photo-detector leads to indistinguishable photo-detection statistics since, for both states, the probability to detect $|0, 2\rangle$ is $\frac{1}{2}$ and the probability to detect $|2, 0\rangle$ is also $\frac{1}{2}$. However, by preceding the detection beam splitter by a single-mode phase shifter (imposing a differential phase shift), one can first transform any of the orthogonal relative phase states to (12), which in turn is transformed to the $|1, 1\rangle$-state. In this way it is possible to implement any transformation $|1, 1\rangle\langle\phi^{(2)}| \exp(-i\phi\hat{n}_{12})$. Subsequent detection of the $|1, 1\rangle$-state allows us to measure the relative phase distribution function defined by (8).

The distribution function for a relative phase eigenstate with eigenvalue zero $P^{(2)}_{|\phi_0^{(2)}\rangle}(\phi)$ can be computed using (8) and (12). We find that $P^{(N)}_{|\phi^{(2)}\rangle}(\phi) = 0$ for $N \neq 2$ and

$$P^{(2)}_{|\phi^{(2)}\rangle}(\phi) = \frac{\sin^2(3\phi/2)}{9\sin^2(\phi/2)}. \quad (14)$$

We note that $P^{(2)}_{|\phi^{(2)}\rangle}(0) = 1$ and $P^{(2)}_{|\phi^{(2)}\rangle}(\pm 2\pi/3) = 0$ since the states $|\phi_{\pm 1}^{(2)}\rangle$ are orthogonal to $|\phi_0^{(2)}\rangle$.

4. Experimental implementation of a relative phase analyser

Figure 1 shows an experimental scheme for measuring the relative phase distribution function in the second manifold. In principle it is possible to make a relative phase eigenstate by just mixing the two modes in a 21.1/78.9% beam splitter and photo-counting the output modes. However, in order to improve the mechanical stability of the interference experiment, we used two orthogonally polarized modes in the same spatial mode instead of two spatially separated modes
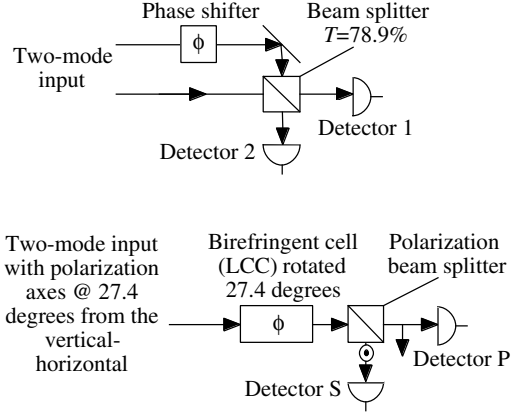
Figure 1. A schematic picture of a relative phase detection setup for the $N = 2$ energy manifold. At the top, in a spatial-mode configuration, at the bottom, in an equivalent polarization-mode configuration.
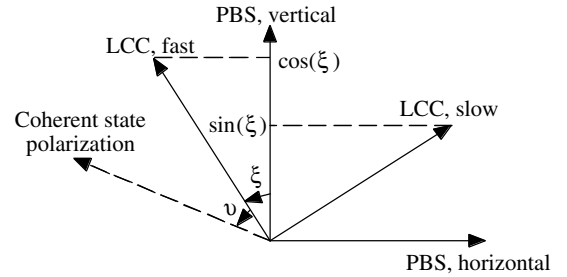
Figure 2. An illustration of the polarization directions of the LCC (which defines the analyser polarization mode basis) and the PBS preceding the photon counters. A rotation ξ of the polarization basis corresponds to a beam splitter transformation with transmittivity $T = \cos^2(\xi)$. In our analyser $\xi = 27.4°$.

of the same polarization. For such an interferometer a beam splitter can be implemented by rotation of the coordinate system by some angle ξ. For example, a 21.1/78.9% beam splitter corresponds to the rotation by $\arccos(1/\sqrt{3})/2 = 27.4°$. It means that a $|1, 1\rangle$-state in the horizontal–vertical polarization basis will be a relative phase eigenstate in a polarization basis rotated 27.4°. We have used this fact to generate such states.

In our first, pulsed experiment, performed in Stockholm, the phase shift was implemented by a variable voltage controlled liquid-crystal birefringent cell (LCC). This cell was inserted with its fast axis at an angle ξ to the vertical direction as shown in figure 2. The LCC subsequently imposes a differential phase shift between the two modes of the impinging two-mode state $|\psi\rangle$. To analyse the state a polarizing beam splitter (PBS) with its principal polarization axis in the horizontal–vertical direction (and hence rotated by $-\xi$ degrees with respect to the LCC fast axis) was placed after the LCC. When ξ is, e.g. $\arccos(1/\sqrt{3})/2 = 27.4°$, the relative phase eigenstate (12) in the fast and slow axis frame of the rotated LCC is transformed to the $|1, 1\rangle$-state in the horizontal–vertical polarization basis. By measuring the photon correlation between the two outputs of the PBS with a pair of single-photon counters (SPCs) the coincidence rate will be proportional to the relative phase distribution function of the state $|\psi\rangle$. If the detectors, the LCC and the PBS
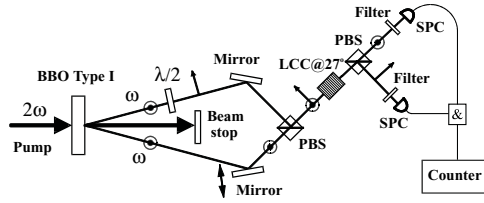
Figure 3. A schematic picture of the experimental setup for the generation of a relative phase eigenstate and detection of its relative phase distribution function with a pulsed-pump laser.

Figure 4. A qualitative illustration of the different timescales involved. The pairwise adjacent pulses represent photon pairs emanating from the same pump pulse. The two pulse pairs separated by τ_{rep} represent photon pairs emanating from subsequent pump pulses. Note that the figure is not drawn to scale.

were ideal, the coincidence count probability would equal the relative phase distribution function.

In our second, cw experiment, performed in Boston, the phase shift was implemented by a birefringent crystalline quartz delay line formed by two quartz wedges assembled so that the light passed a variable thickness quartz 'plate'. In this experiment it was difficult to rotate the two quartz wedges for mechanical reasons, so instead we rotated the $|1, 1\rangle$-state by $27.4°$ by the means of a $\lambda/2$-plate rotated by half that angle.

5. Measurements of the relative phase distribution function

We have implemented the procedure outlined above to provide the first experimental confirmation of a relative phase operator of the type suggested by Luis and Sánchez-Soto. We have made measurements on two different kinds of states: relative phase eigenstates and two-mode coherent states.

5.1. The relative phase distribution function of a short pulse relative phase eigenstate

The generation of the state (12) is illustrated in figure 3. A two-photon $|1, 1\rangle$-state is created by spontaneous degenerate parametric down-conversion. The light source was a Ti–Sapphire laser pumped with an Ar laser. A pulse-train of 100 fs long pulses at a repetition frequency of 80 MHz of 780 nm IR light was first frequency doubled and subsequently frequency down-converted to generate vertically polarized photon pairs. This generation scheme is standard practice [18–20]. BBO nonlinear crystals with type-I phase matching were used for both the frequency doubling and the down-conversion (a 0.5 mm crystal for the doubling and a 3.0 mm crystal for the down-conversion). Direct detection of the photon pairs gave typical average counting rates for the detectors of $10\,000$ s^{-1}. That rate corresponds to a 1.25 s^{-1} random coincidence rate. The detectors' dark current count-rate was 20 s^{-1}. Two similar 780 nm interference filters with 10 nm passband were placed in front of the detectors. Irises were used for single-mode transverse selection.

The frequency degenerate photon pairs were generated in two modes that formed equal but opposite angles with respect to the pump beam. The polarization of one mode was rotated from vertical to horizontal polarization by a half-wave plate. The two photons were then spatially overlapped in a PBS. One of the PBS output ports gave the $|1, 1\rangle$-state in the horizontal–vertical polarized basis. In the basis of the LCC the state (12) was created since the LCC was mounted at an angle $\xi = 27.4°$
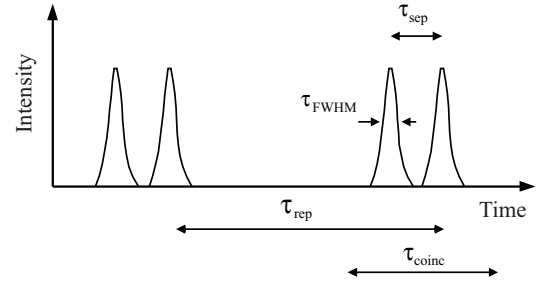
to the vertical direction, as discussed in section 4 above. In order to maximize the spatial overlap of the two modes, one of the mirrors (indicated by the double arrow in figure 3) was placed on a Melles Griot nanopositioner with 50 nm linear displacement resolution.

The correlation between the two outputs of the second PBS was measured with a pair of EG&G SPCs, a home-built correlation AND circuit and a HP53131A counter. A typical coincidence rate was 20 s^{-1}. The time coincidence window τ_{coinc} was set to 3 ns, short enough to exclude the random coincidence between photons generated by subsequent pump pulses. (The pump-pulse separation τ_{rep} was 12.5 ns.) On the other hand, the time coincidence window was longer than the detector jitter (200 ps) and much longer than the photon-pair wavefunction τ_{FWHM} (which was about 50 fs). By moving the mirror mounted on the nanopositioner, the time separation τ_{sep} between the vertically and horizontally polarized input pulse could be varied by ± 250 ps in steps of 0.3 fs. The different timescales are schematically shown in figure 4.

Ideally (when the mode functions overlap perfectly) the photon correlation is proportional to (14). This result is plotted as a dashed curve in figure 5. As is clear from the figure, and the analysis above, the states with $\phi = 0$, $\phi = 2\pi/3$, and $-2\pi/3$ are mutually orthogonal and therefore the 'visibility' is unity in this case. (We have defined the 'visibility' in the standard way as $(I_{max} - I_{min})/(I_{max} + I_{min})$. Note that some authors refer to the quantity $1 - I_{min}/I_{max}$ as the visibility.) The experimental points are shown as black dots in the figure. The dot size corresponds roughly to the stochastic experimental error-bars. The main difference between the experimental and the theoretical curve is the smaller 'visibility' (45%) in the experimental data. To explain this we note that our choice of timescales ($\tau_{rep} > \tau_{coinc} \gg \tau_{sep}, \tau_{FWHM}$) means that even if the two photons' mode functions do not overlap perfectly, or even do not overlap at all but are within the time coincidence window, they can give rise to coincidence-counter clicks. We are quite confident that the nonperfect mode-function overlap is the main source of nonunity 'visibility' in figure 5, since the measurements on two-mode coherent states (see below) whose wavefunctions overlapped almost per definition, gave a much better fit with theory. Let us examine the latter case (strictly nonoverlapping pulses) first.

If the two orthogonally polarized photon pulses have nonoverlapping mode functions, no interference between
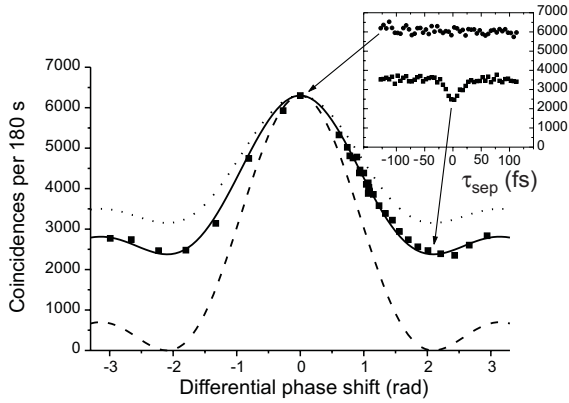
Figure 5. The computed (dashed curve) and the measured (solid curve) relative phase distribution function for the pulsed relative phase eigenstate. The dotted curve corresponds to the theoretical result for two classical noninterfering particles. The inset shows the transition between interfering and noninterfering pulses for the differential phase shifts $\phi = 0$ and $\phi = 2\pi/3$. The pulses impinging on the interferometer were displaced in time using a movable mirror.

them can take place. In this case we can treat the propagation of the two photons through the setup separately. The $|1, 0\rangle$ input state will have some probability $P_{1t}(\phi)$ to exit the rightmost PBS in figure 3 in the same state and the probability $1 - P_{1t}(\phi)$ to exit the PBS in the state $|0, 1\rangle$. Similarly, we can define the probability $P_{2t}(\phi)$ for the $|0, 1\rangle$ input state. If the two photons leave the PBS in different ports, our coincidence detector will record them as coincident although they do not overlap ($\tau_{\text{coinc}} \gg \tau_{\text{sep}} > \tau_{\text{FWHM}}$). The probability for such coincidences is $P_{1t}(\phi)P_{2t}(\phi) + (1 - P_{1t}(\phi))(1 - P_{2t}(\phi))$. Computing this probability one gets

$$\left(1 + \frac{\sin^2(3\phi/2)}{9\sin^2(\phi/2)}\right)\bigg/ 2. \tag{15}$$

This function is plotted as the dotted curve in figure 5. One sees that this function is a displaced and rescaled copy of (14). However, the 'visibility' in this case is $\frac{1}{3} \approx 33\%$. This value of the 'visibility' delineates the border between classical versus quantum explanation models for the experiment and clearly shows that our experiment is a manifestation of a quantum interference effect.

Note that we have used the words 'mode-function overlap' in the broadest sense. It does not simply refer to the transverse mode-function overlap but refers to overlap in all of phase space. Earlier reports have shown that it is difficult to achieve good mode-function overlap for sub-ps pulses due to the pump-pulse frequency spread and the group-velocity dispersion in the BBO crystal [18, 21, 22]. We are convinced that our poor overlap depends on a combination of the real-space and linear momentum-space overlap. In the following section we show how a quasi-continuous generation of the same states lead to a significantly better 'visibility'.

In fact it is possible to check that the relative phase distribution is a manifestation of interference by spatially separating the two pulses impinging on the leftmost PBS along the propagation direction (through the movable mirror). As explained above, if $\tau_{\text{coinc}} > \tau_{\text{sep}} > \tau_{\text{FWHM}}$ the photodetectors will still be able to record coincidence counts

from strictly noninterfering photons. The transition from interfering to noninterfering photons is shown in figure 5, inset, for two different values of the differential phase shift ϕ. At the setting $\phi = 0$, the fast and the slow axis in the LCC are degenerate (they give the same phase shifts), so the $|1, 1\rangle$-state (in the horizontal–vertical basis) remains in the same state until it impinges on the rightmost PBS. If the mode functions of the vertically and horizontally polarized mode are separated, the $|1, 0\rangle$-state and the $|0, 1\rangle$-state likewise remain in their respective states and will be recorded as coincident as long as $\tau_{\text{coinc}} > \tau_{\text{sep}}$. Therefore, the coincidence rate for this setting of ϕ should be independent of the mode-function overlap as long as $\tau_{\text{coinc}} > \tau_{\text{sep}}$. This is in agreement with the experimental data (inset in figure 5, where the vertical axis is identical to the main figure).

When ϕ is set to $2\pi/3$, there will be a difference in the coincidence rate depending on whether the two photons' mode functions overlap or not. The coincidence rate for non-overlapping modes will be half as large as the rate at $\phi = 0$, and the rate for perfectly overlapping modes will be zero due to quantum interference. In our experiment we see a substantial reduction in the coincidence rate when the path-length difference between the down-conversion BBO crystal and the LCC is zero. The width of the coincidence dip in the inset corresponds well to the convolution of two Gaussian pulses with $\tau_{\text{FWHM}} = 50$ fs. Therefore, we believe that the main source of nonunity 'visibility' is that our photon pairs are not perfectly overlapping. Losses (i.e. absorption of one or both the photons), on the other hand, will simply decrease the rate of coincidences for all settings of the LCC. Assuming that our state can be described as a mixed state of overlapping and nonoverlapping pulses, we have plotted the solid curve which is a probability weighted sum of (14) and (15). This curve fits well with the experiment. We stress that figure 5 represents the raw data. That is, no base-line correction or subtraction of dark counts has been undertaken.

5.2. The relative phase distribution function of a quasi-cw relative phase eigenstate

To confirm that it was experimental limitations and not any intrinsic flaw of the theory which caused the moderate 'visibility' results for our pulsed light experiment we repeated the experiment with a quasi-cw pump source. Comparing the obtained results with the results presented above gives a good illustration of the difficulties associated with the higher-order polarization dispersion of pulsed entangled photon-pair sources [18, 21, 22]. The light source in the quasi-continuous experiment was a single-mode cw Ar laser with a wavelength of 351.1 nm. The generation of the state (12) is illustrated in figure 6. A two-photon $|1, 1\rangle$-state with orthogonal polarizations was created by degenerate type-II spontaneous parametric down-conversion. This generation scheme too is standard practice [23]. A 0.5 mm BBO nonlinear crystal with type-II phase matching was used for the down-conversion. The frequency degenerate photon pairs were generated co-linearly in a single spatial mode. Due to the *linear* dispersion of the crystal, the horizontally and vertically polarized photons are separated in time. A birefringent crystalline quartz delay line between the horizontal and vertical basis
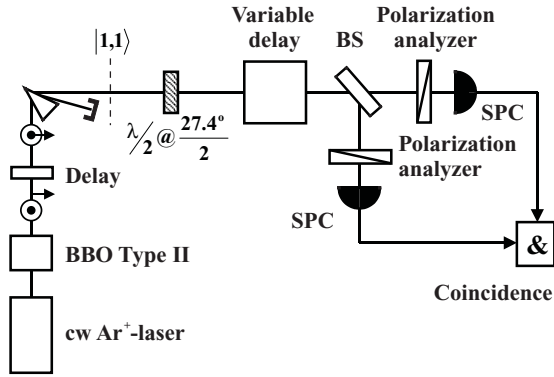
Figure 6. A schematic picture of the experimental setup for the generation of a relative phase eigenstate and detection of its relative phase distribution function using a cw pump laser.

Figure 7. The computed relative phase distribution function (solid curve) and the experimental data (dots) for the quasi-cw relative phase eigenstate.

was used to compensate for the linear dispersion, which made the two orthogonally polarized photons overlap in time [24]. Direct detection of the photon pairs gave typical average counting rates for the detectors of 5000 s^{-1}. That rate corresponds to a 0.075 s^{-1} random coincidence rate within the chosen coincidence detection window $\tau_{\text{coinc}} = 3$ ns. The detectors' dark current count-rate was 50 s^{-1}. Two similar 702.2 nm interference filters with 80 nm bandwidth were placed in front of the detectors. The filter bandwidth was much larger than the bandwidth involved in the parametric down-conversion process and thus only ambivalent light was filtered. Irises were used for single-mode transverse selection.

A $\lambda/2$-plate mounted at an angle $\xi = 27.4°/2$ to the vertical direction rotated the polarization of the photons and created the state (12). The differential phase shift was applied by adjusting another birefringent crystalline quartz delay line (see figure 6). The state was thereafter split by a beam splitter. The analysers at the output of the beam splitter were set to 27.4° and $(27.4 + 90)$° respectively. The correlation between the two outputs of the beam splitter were measured with a pair of EG&G SPCs, a EG&G time-to-amplitude converter and a EG&G three-channel counter. A typical coincidence rate was 10 s^{-1}.

The result of this experiment is plotted in figure 7. The experimental data presented is just as collected (raw data) without any background subtraction. It can be seen that the 'visibility' is much higher (about 90%) and the agreement with theory is substantially better in this experiment than in the pulsed light experiment since the bandwidth, and hence dispersion, of the generated photon pairs was much smaller.

5.3. The relative phase distribution function of two-mode coherent states

Removing the nonlinear crystal from the pulsed light setup allowed us to make measurements of $P_{|\psi\rangle}^{(2)}(\phi)$ for two-mode coherent states. Different two-mode coherent states $|\alpha \cos(\upsilon), \alpha \sin(\upsilon)\rangle$ were produced by rotating the polarization of a linearly polarized coherent state $|\alpha, 0\rangle$ an angle υ relative to the fast axis of the LCC. (Remember that the LCC principal axis defines the polarization basis axes of our relative phase analyser.) The main restriction with the
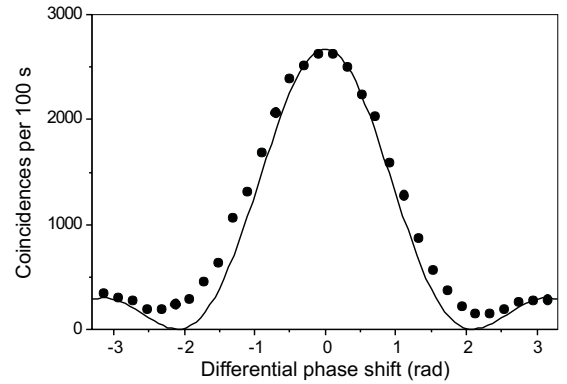
present scheme is that only states with a low average total photon number can be measured since the detection scheme is based on single-photon detectors that cannot distinguish between one and more than one photon. The probability of detecting two or more photons relative to the probability of detecting a single photon can be made arbitrarily low by attenuating the coherent state. The Ti–Sapphire laser described above was attenuated to a mean photon number per pulse of 0.004. Hence, the probability of detecting one photon was about 500 times greater than the probability of detecting two, or more, photons in a pulse. A $\lambda/2$-plate was used to rotate the vertically polarized attenuated laser light to linearly polarized light with a variable polarization direction υ (see figure 2), corresponding to certain excitation amplitudes for the coherent states in the fast and slow axis frame of the LCC. The relative phase distribution function could thereafter be measured as described previously.

Figure 8 shows the results for two-mode coherent states with low mean photon number. The rotation angles used were $\upsilon = -\xi = -27.4°$, $\upsilon = 0$ and $\upsilon = \pi/4$. The expressions for the theoretical curves are given by

$$P_{|\psi\rangle}^{(2)}(\phi) = \frac{\sin^2(\frac{\phi}{2})(8 + 4\cos(\phi))}{9} \qquad \text{for} \quad \upsilon = -\xi, \quad (16)$$

$$P_{|\psi\rangle}^{(2)}(\phi) = \tfrac{1}{3} \qquad \text{for} \quad \upsilon = 0, \quad (17)$$

and

$$P_{|\psi\rangle}^{(2)}(\phi) = \frac{2 - \cos(2\phi)}{6} \quad (18)$$

for $\upsilon = \pi/4$. It is worth noticing that for the setting $\upsilon = 0$ the relative phase of the state $|\alpha, 0\rangle$ is recorded. As expected, the relative phase distribution is flat, as it is for any product state where one of the constituent states is the vacuum or a number state. The setting $\upsilon = \pi/4$ gives the relative phase analyser input state $|\alpha/\sqrt{2}, \alpha/\sqrt{2}\rangle$. Finally, the setting $\upsilon = -\xi$ gives the only state which is orthogonal to any of the relative phase analyser eigenstates. In the second manifold this state is in a linear superposition of the states $|\phi_{-1}^{(2)}\rangle$ and $|\phi_1^{(2)}\rangle$. Hence, $P_{|\psi\rangle}^{(2)}(0) = 0$.

We attribute the differences between the measurement points and the theoretical curves to the somewhat poor precision ($\pm 1°$) in the setting of the angle of rotation υ. This is particularly apparent for the setting $\upsilon = 0$. If
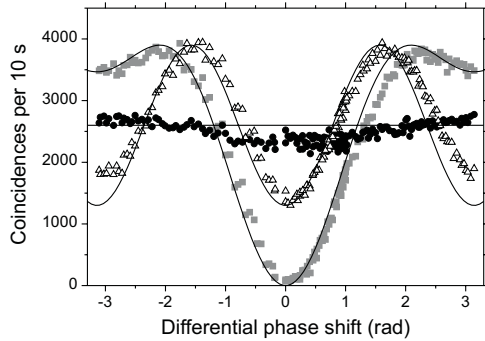
Figure 8. The computed and the measured relative phase distribution functions for two-mode coherent states. The squares correspond to the setting $\upsilon = -\xi$, the triangles to $\upsilon = \pi/4$, and the filled circles to $\upsilon = 0$.

the attenuated coherent state polarization was truly parallel with the LCC fast axis, then the coincidence count-rate would be independent of ϕ. Instead we see a slight U-curve which indicates that the polarization is off its intended value by about $1.3°$. We are presently replacing our manual polarization rotator with a high-precision digitally controlled one and this should reduce this systematic error in future experiments. Another error term is that neither of the PBSs used are ideal. The measured reflectivity for S-polarized light is 99.3% and the transmittivity for P-polarized light is 96.2%. This slightly distorts the experimental data in a state-dependent fashion. We reiterate that the experimental points in figure 8 are uncorrected data and that a correction of either the theory to account for the imperfections in the experimental setup, or of the data to compensate for the experimental imperfections, results in a substantially better fit between the predicted curve and the experimental points.

Yet, the results are in much better agreement with theory than for the pulsed relative phase states. The reason is that a linearly polarized TEM_{00} single-mode (whether pulsed or cw) coherent state per definition factorizes into a two-mode coherent state with identical mode functions in a rotated polarization basis. This is in contrast to the state $|1, 1\rangle$ in which the two photons must be in identical, but $\pi/2$ rotated, spatial modes in order for a polarization basis rotation to be equivalent to a beam splitter transformation. By using irises and filters we can coerce the transverse mode of the down-converted photons into similar modes, but due to the fact that the BBO crystal is not cut at $90°$ to the principal axis, we have a slight horizontal asymmetry in the pulsed down-conversion setup which, in combination with group-velocity dispersion (remember that $\tau_{FWHM} = 50\,\text{fs}$), degrade the mode overlap.

6. Discussion and conclusions

We have experimentally implemented a two-mode relative phase measurement in the second excitation manifold and we have measured the relative phase distribution of a relative phase eigenstate and for two-mode coherent states.

In our analyser we can only project onto one relative phase state at a time, while in an ideal analyser in the second manifold, one would project onto all three orthogonal relative

phase states simultaneously. However, in order to do so, a nonlinear differential phase shifter is needed and such a component is not quite in reach at the two-photon excitation level with present technology. Therefore we have resorted to linear components (a birefringent variable phase shifter or a birefringent delay line, and a PBS) and paid the price of only projecting onto one relative phase state at a time.

We note that since only linear components are used, our experiment can be interpreted as an unbalanced two-photon interferometer experiment. With this view, our rather involved relative phase formalism is not needed to predict the outcome of the experiment. (It is of course generally true that the dynamics of any physical system can be fully described in any complete orthonormal basis spanning the pertinent Hilbert space.) To describe interferometers it is convenient to use the relative phase states since the phase-evolution operator transforms these states in a particular simple way. Moreover, had we had the technology to implement the full unitary transformation (9), then it would not even have been possible to describe the experiment in terms of a (linear) interferometer. Hence, our experiment should be seen as a proof of principle confirmation of the Hermitian two-mode relative phase operator.

The second limitation in our experiment is that our analyser only works in the second manifold. This is again due to the entangled character of the relative phase eigenstates. In order to implement the full transformation (9) a nonlinear Hamiltonian is needed [15]. Therefore, future work on the relative phase operator will have to focus on approximate implementations. Nonetheless, it is our firm belief that the relative phase operator constructed by Luis and Sánchez-Soto, and generalized by us, still provides a useful theoretical description of the two-mode quantum relative phase, with which one can rigorously analyse any phase sensitive system such as phase modulated fibre-optical communication systems or interfering Bose–Einstein condensed multi-atom states [25–27].

Acknowledgments

References

[1] London F 1926 *Z. Phys.* **37** 915
London F 1927 *Z. Phys.* **40** 193
[2] Dirac P A M 1927 *Proc. R. Soc.* A **114** 243
[3] Louisell W H 1963 *Phys. Lett.* **7** 60
[4] Susskind L and Glogower J 1964 *Physics* **1** 49
[5] Carruthers P and Nieto M M 1968 *Rev. Mod. Phys.* **40** 411
[6] Pegg D T and Barnett S M 1988 *Europhys. Lett.* **6** 483
Barnett S M and Pegg D T 1996 *Phys. Rev. Lett.* **76** 4148
[7] Noh J W, Fougères A and Mandel L 1992 *Phys. Rev.* A **45** 424
Fougères A, Monken C and Mandel L 1994 *Opt. Lett.* **19** 1771
Torgersson J R and Mandel L 1996 *Phys. Rev. Lett.* **76** 3939

[8] Lynch R 1995 *Phys. Rep.* **256** 367
[9] Tanas R, Miranowicz A and Gantsog Ts 1996 *Progress in Optics* vol 35, ed E Wolf (Amsterdam: North-Holland) p 355
[10] Pegg D T and Barnett S M 1997 *J. Mod. Opt.* **44** 225
[11] Fujikawa K 1995 *Phys. Rev.* A **52** 3299
[12] Luis A and Sánchez-Soto L L 1993 *Phys. Rev.* A **48** 4702
     Luis A and Sánchez-Soto L L 1994 *Opt. Commun.* **105** 84
     Luis A and Sánchez-Soto L L 1996 *Phys. Rev.* A **53** 495
     Luis A and Peřina J 1996 *Phys. Rev.* A **54** 4564
[13] Ban M 1991 *J. Math. Phys.* **32** 3077
     Ban M 1993 *Phys. Rev.* A **48** 3452
[14] Yu S 1997 *Phys. Rev. Lett.* **79** 780
[15] Björk G and Söderholm J 1999 *J. Opt. B: Quantum Semiclass. Opt.* **1** 315
[16] Yu S 1997 *Phys. Rev.* A **56** 3464
[17] Grangier P, Roger G and Aspect A 1986 *Europhys. Lett.* **1** 173
[18] Di Giuseppe G, Haiberger L, De Martini F and Sergienko A V 1997 *Phys. Rev.* A **56** R21
[19] Grice W P, Erdmann R, Walmsley I A and Branning D 1998 *Phys. Rev.* A **57** R2289
[20] Pan J W, Bouwmeester D, Weinfurter H and Zeilinger A 1998 *Phys. Rev. Lett.* **80** 3891
[21] Joobeur A, Saleh B E A, Larchuk T S and Teich M C 1996 *Phys. Rev.* A **53** 4360
[22] Atatüre M, Sergienko A V, Jost B M, Saleh B E A and Teich M C 1999 *Phys. Rev. Lett.* **83** 1323
[23] Kiess T E, Shih Y H, Sergienko A V and Alley C O 1993 *Phys. Rev. Lett.* **71** 3893
     Shih Y H, Sergienko A V, Rubin M H, Kiess T E and Alley C O 1994 *Phys. Rev.* A **50** 23
[24] Rubin M H, Klyshko D N, Shih Y H and Sergienko A V 1994 *Phys. Rev.* A **50** 5122
[25] Leggett A J and Sols F 1991 *Found. Phys.* **21** 353
[26] Andrews M R, Townsend C G, Miesner H J, Durfee D S, Kurn D M and Ketterle W 1997 *Science* **275** 637
[27] Marburger J H III and Das K K 1999 *Phys. Rev.* A **59** 2213